Predictions of the Thermodynamic Properties of Multicomponent Polyolefin Blends from Measurements on Two-Component Systems

H. S. Jeon, J. H. Lee, and N. P. Balsara*

Department of Chemical Engineering, Chemistry, and Materials Science, Polytechnic University, Six Metrotech Center, Brooklyn, New York 11201

Received July 1, 1997; Revised Manuscript Received March 4, 1998

ABSTRACT: Scattering experiments were conducted on a critical, binary mixture of polyethylene (PE) and head-to-head polypropylene (PP), and a symmetric PE−PP diblock copolymer melt. The binary mixture exhibited a liquid−liquid phase transition at 143 °C, while the block copolymer exhibited an order−disorder transition at 149 °C. Estimates of the Flory−Huggins interaction parameter between PE and PP, and the statistical segment lengths of the chains were obtained by fitting neutron scattering profiles from the PE/PP blends and the PE−PP block copolymer, in the single-phase regime, to theoretical predictions based on the random phase approximation (RPA). These estimates were used to compute the scattering profiles of multicomponent blends comprising PE, PP, and PE−PP. A phase diagram for these blends was constructed on the basis of the computed scattering profiles. In the paper that follows this one, we compare the theoretical computations with experimental data from multicomponent PE/PP/PE−PP blends.

Introduction

Studies of multiphase polymer systems are motivated, in part, by their technological importance. It is well-known that the properties of these materials are inextricably linked to the morphology of the phases.[1] Hard materials with enhanced toughness are obtained by incorporating a dispersed rubbery macrophase in glassy and crystalline materials such as polystyrene and Nylon.[2] On the other hand, soft materials, suitable for the production of gaskets and adhesives, are based on microphase-separated block copolymers.[3] The term macrophase is used to describe domains that are much larger than molecular dimensions, while the term microphase is used to describe domains with sizes that are comparable to molecular dimensions.

Binary homopolymer blends have served as model systems for studying macrophase separation. The characteristics of concentration fluctuations in single-phase blends, in the vicinity of the phase separation temperature, have been studied by neutron scattering.[4−7] The scattering profiles from these systems are devoid of peaks (at finite scattering angle), indicating that the distribution of length scales associated with the concentration fluctuations is broad. The scattering intensity maximum occurs in the forward direction, i.e., as the scattering angle tends to zero. This implies the presence of fluctuations with characteristic lengths that are much larger than molecular dimensions. When phase separation is induced in these systems, the resulting two-phase morphology has many of the characteristics of the concentration fluctuations. A wide distribution of phase sizes is usually observed,[8,9] and there is no theoretical upper limit on the size of the phases. Coarsening continues until the phase size is limited by the size of the container.

Block copolymer melts have served as model systems for studying microphase separation. The characteristics of concentration fluctuations in the single-phase regime are qualitatively different from those found in binary blends. The scattering profiles exhibit a peak at finite scattering angles.[10,11] This implies the presence of a characteristic length scale for the concentration fluctuations that is roughly equal to the unperturbed dimension of the molecule.[12] In addition, the scattered intensity in the forward direction is zero, implying that there are no fluctuations with large length scales. Upon phase separation, block copolymers form ordered microphases and show no evidence of macrophase separation.[13]

We therefore see that, in both binary homopolymer blends and block copolymer melts, the concentration fluctuations in the single-phase regime are announcements of the nature of the impending phase transition. This is typical of systems undergoing weak first-order and second-order phase transitions.[14]

Mean-field theories based on the random phase approximation (RPA) provide a unified framework for studying concentration fluctuations near macrophase and microphase transition points. This approximation was originally invoked by de Gennes to describe concentration fluctuations in binary polymer blends.[5] The wide applicability of the RPA became evident after Leibler's seminal work on block copolymer melts.[12] More recently, Benoit et al.[15] and Akcasu et al.[16,17] have extended these ideas, and the RPA can now be applied to any multicomponent polymer mixture, regardless of the number of components and their architectural complexity. An attractive feature of RPA-based theories is that the scattering profiles can be predicted if the Flory−Huggins interaction parameter between components (χ) and the statistical segment lengths (i.e., the scaling of the unperturbed radius of gyration with molecular weight) are known. Tabulations of these quantities may be found in refs 18 and 19.

Our objective is to examine concentration fluctuations and phase transitions in multicomponent blends of two homopolymers and a block copolymer. The polymers used in this study are model polyolefins: polyethylene

S0024-9297(97)00971-6 CCC: $15.00
Published on Web 04/29/1998

(PE), head-to-head polypropylene (PP), and a symmetric PE−PP diblock copolymer. Experiments were conducted at temperatures between 114 and 167 °C. All the components are rubbery and amorphous in this temperature range. In this paper, which we refer to as paper I, we present the results of scattering experiments on binary PE/PP blends and the PE−PP block copolymer. Neutron-scattering measurements from single-phase systems were used to estimate χ and the statistical segment lengths. Light scattering was used to confirm the location of the liquid−liquid phase transition in the binary PE/PP blend. We then use multicomponent RPA to compute scattering profiles for a series of PE/PP/PE−PP blends. Of course, these calculations are restricted to temperatures at which the multicomponent blends are single phase. We assumed that the nature of the phase transitions in the multicomponent systems can be deduced from these scattering curves, which are indicative of the characteristics of the concentration fluctuations in the single-phase regime. Multicomponent blends with scattering maxima in the forward direction are assumed to undergo macrophase separation, while those with scattering peaks at finite angles are assumed to undergo microphase separation. This enables us to predict the phase diagram for PE/PP/PE−PP blends. In paper II,[20] which follows the present paper, we compare these predictions with experimental measurements on PE/PP/PE−PP blends.

The locus of points that divides the macrophase-separated states from the microphase-separated states is called the Lifshitz line. Thermodynamic studies in the vicinity of the Lifshitz line were conducted by Zin and Roe, who studied mixtures of one homopolymer and a block copolymer, using light and X-ray scattering.[21,22] Ramos and Cohen used electron microscopy to show that mixtures of two homopolymers and a block copolymer could exhibit either macrophase separation or microphase separation.[23] Recent studies on the thermodynamics of homopolymer/homopolymer/block copolymer mixtures have been carried out by Bates et al.[24] and Jackson et al.[25] Theoretical calculations demonstrating the complexity of phase behavior of these multicomponent blends were conducted by Leibler,[26] Broseta and Fredrickson,[27] and Holyst and Schick.[28] Broseta and Fredrickson showed that under some conditions, the Lifshtiz line ends in a Lifshtiz point. Experimental evidence for the existence of such a point was provided by Bates et al.[24]

This paper and paper II[20] are part of a series on the thermodynamics of multicomponent blends.[29−34] In earlier work, we compared multicomponent RPA predictions with neutron scattering data from mixtures of poly(methylbutylene), poly(ethylbutylene), and poly(methylbutylene)-*block*-poly(ethylbutylene). These blends were relatively simple and exhibited scattering maxima in the forward direction, in the single-phase regime, over the entire range of temperatures, compositions, and component molecular weights that were examined.[29,30] In addition, the scattering profiles were in quantitative agreement with multicomponent RPA predictions without any adjustable parameters. We also examined the early stages of macrophase separation in these systems in both the nucleation and growth[31] and spinodal decomposition[32] regimes. In another study, we examined the effect of molecular architecture on the thermodynamics of pure block copolymers.[33] We compared scattering data from melts of complex block copolymers such as an asymmetric polystyrene-*block*-polyisoprene-*block*-polystyrene copolymer with that from conventional diblock copolymers. In this case, only qualitative agreement with multicomponent RPA was obtained. More recently, we studied the structure of PE/PP/PE−PP blends wherein the homopolymer molecular weights were an order of magnitude larger than those used in the present study.[34] These blends were strongly phase separated and outside the realm of the RPA. We were interested in domain shape transitions (e.g. spherical-to-cylindrical dispersions), that were predicted by equilibrium theories of Leibler[35] and Wang and Safran.[36] In contrast to theoretical predictions, we found a transition from spheres to cell-like domains, and the cell-like domains appeared to be out of equilibrium.[34]

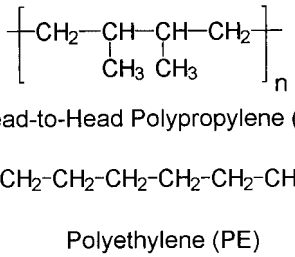

Figure 1. Chemical structure of monomers of head-to-head polypropylene (PP) and polyethylene (PE) chains.

Experimental Section

Model polyolefins were derived from anionically polymerized dienes.[37] Polyethylene (PE) was obtained from 1,3-butadiene (Matheson Gas Products), while head-to-head polypropylene (PP) was obtained from 2,3-dimethyl-1,3-butadiene (Aldrich Chemical Co.). Polymerization was carried out under high vacuum, in cyclohexane, with *sec*-butyllithium as the initiator and 2-propanol as the terminator. Standard high vacuum procedures were used to purify the reagents.[38] Polybutadiene was synthesized at room temperature, and the reaction mixture was left to stand for 2 days before termination. Poly(dimethylbutadiene) was synthesized at a slightly elevated temperature (35 °C) because the polymer is crystalline at temperatures below 30 °C. This reaction proceeds rather slowly, and 5 days was required for completion. A polybutadiene-*block*-poly(dimethylbutadiene) copolymer was synthesized by sequential polymerization of 1,3-butadiene followed by 2,3-dimethyl-1,3-butadiene, under conditions described above.

Separate aliquots of the polydienes were saturated with H_2 and D_2 to yield fully hydrogenated and partially deuterated polyolefins. The saturation reaction was carried out in a high-pressure batch reactor (Parr Instrument Co.), using heterogeneous catalysis with $Pd/BaSO_4$ (Stern Chemical Co.), at 100 °C and 400 psig. The saturation step was repeated until the C=C signatures could not be detected in the IR and ^1H and ^{13}C NMR spectra. After the reaction was complete, the hot solution was filtered several times to remove the catalyst particles. The last filtration was through a 0.22 μm filter (Anodisc). The chemical structure of the PE and PP chains is shown in Figure 1.

The characteristics of the polymers used in this study were determined by methods given in refs 29, 30, and 34 and are listed in Table 1. The composition of the homopolymers and copolymer was determined from ^{13}C NMR measurements. The polydiene chains were statistical copolymers, composed of 1,2 and 1,4 isomers. The percentage of 1,4 isomers was 93% for the polybutadiene chains and 95% for the poly(dimethylbutadiene) chains, irrespective of whether the chains were homopolymers or parts of the block copolymer. The volume fraction of PE units in the PE−PP copolymer was 0.49. DSC measurements on the PE and PE−PP, at a heating rate of 10

Table 1. Characteristics of Polyolefins

sample designation	mol wt (wt av)[a] (kg/mol)	polydispersity index[b]	vol fr of PE in block copolymer[c]	density[d] (g/cm^3)	av no. of deuterium per C_6 monomer[e]
hPE	7.0	1.04		0.9275	0
dPE	7.4	1.04		0.9865	5.24
hPP	15	1.10		0.8744	0
dPP	16	1.09		0.9321	5.43
hPE−hPP	63	1.12	0.49	0.8973	0
dPE−dPP	66	1.12	0.49	0.9476	4.51

[a] From light scattering from dilute solutions of polydienes. [b] From high-temperature GPC. [c] Based on ^{13}C NMR. [d] From density measurements using a density gradient column. [e] Based on density measurements.

°C/min, revealed a crystalline melting transition between 107 and 110 °C. The PP homopolymer is amorphous at room temperature.

Mixtures were prepared by solution blending. We started with a dilute solution (1 wt % total polymer) containing the appropriate amounts of the components in toluene. The mixture was stirred and heated from room temperature to 108 °C in 90 min, at which point the toluene began to boil. All the polymers were soluble in boiling toluene. The mixture was kept at 108 °C for 15 min and then poured quickly into a 50/50 methanol/acetone mixture at room temperature. This resulted in the formation of a white precipitate. About 0.25 g of the precipitate was transferred on to a quartz disk (ca. 1.0 mm in thickness and 23 mm in diameter) with an aluminum spacer (1.0 mm thick, 23 mm outer diameter and 16 mm inner diameter) and heated to 200 °C in a vacuum oven. This caused the blend to flow and occupy the space provided by the spacer. The blend was then capped by slowly pressing another quartz disk, until a sample with uniform thickness was obtained. These samples were used in both neutron- and light-scattering experiments.

The small angle neutron scattering (SANS) experiments reported in this paper were conducted on the 8 m SANS machine (on the NG5 beam line) at the National Institute of Standards and Technology in Gaithersburg, MD. Two-dimensional SANS patterns were measured using the following instrument configuration: neutron wavelength, $\lambda = 12.0$ Å, wavelength spread $\Delta\lambda/\lambda = 0.25$, sample-to-detector distance = 3.6 m, sample aperture = 1.2 cm, source-to-sample distance = 4.1 m, and source size = 2.7 cm. The measured data were converted to absolute scattering intensity using secondary standards described in ref 29. The scattering profiles from the samples were azimuthally averaged and corrected for background scattering, empty cell scattering, and detector sensitivity. In one particular experiment (on pure dPE−dPP) the sample was purposely perturbed, and this resulted in an azimuthally asymmetric scattering pattern. This is the only case where the data were not azimuthally averaged. The incoherent scattering for each blend was estimated from SANS measurements on a pure, fully hydrogenated polyolefin, assuming that it is proportional to the H-atom concentration in the blend. The total scattered intensity was also corrected for scattering due to nonuniformity of deuterium labeling in the partially deuterated homopolymer chains present in the blend.[39] The coherent SANS intensity, $I(q)$ ($q = 4\pi \sin(\theta/2)/\lambda$, where θ is the scattering angle), is given by

$$I(q) = [I(q)]_{\text{measured}} - I_{\text{incoherent}} - \phi_{\text{d,h}} I_{\text{c,h}}(q) \qquad (1)$$

where $I_{\text{c,h}}(q)$ is the measured coherent SANS intensity of the pure partially deuterated homopolymer and $\phi_{\text{d,h}}$ is its volume fraction in the blend. Both corrections were relatively small; the coherent scattering intensity from the deuterated homopolymers was less than 0.5 cm^{-1} in the accessible q range. The coherent scattering intensity from the blends was thus obtained from the raw data without resorting to any adjustable parameters. The scattering profiles were obtained in the temperature range between 114 and 167 °C, and the samples were studied as a function of decreasing temperature. All the blends studied here were single-phase at 167 °C. Samples were equilibrated for at least 30 min at each temperature before starting the measurements.

Small angle light scattering (SALS) was conducted on an apparatus described in ref 32. The sample holder was designed so that samples used in the SANS experiments could be used. A beam of light from a 10 mW He−Ne laser with a wavelength $\lambda = 633$ nm was directed through the sample, which was housed in an electrically heated aluminum block. The scattered light in the angular range from 2.5° to 10.7° (corresponding to q values ranging from 4.33×10^{-5} to 1.85×10^{-4} Å^{-1}) was focused onto a photodetector, using a lens and a beam stop, and recorded as a function of time.

Theoretical Calculations

In this section we present the RPA-based scattering equations for mixtures of two homopolymers and a block copolymer. These equations are identical to those presented in our previous papers.[29,30] However, the calculated scattering profiles for PE/PP/PE−PP blends presented in this paper are qualitatively different from those reported in refs 29 and 30, due to differences in the magnitude of the Flory−Huggins interaction parameter.

In the random phase approximation, the coherent scattering intensity from a single-phase, $(n + 1)$ component, incompressible mixture, $I(q)$, is given by[5,12,15−17,40,41]

$$I(q) = \mathbf{B}^{\mathrm{T}} \underline{\underline{S}}(q) \mathbf{B} \qquad (2)$$

where $\mathbf{B}$ is an n-dimensional column vector whose elements, B_i, are related to the scattering length densities of the components and $\underline{\underline{S}}(q)$ is an n by n structure factor matrix whose elements, S_{ij}, describe correlations between components i and j. A component is defined to be a connected chain of identical monomers. We ignore the fact that the PE and PP chains are actually statistical copolymers. This is appropriate because the RPA in polymer mixtures is based on a coarse-grained view of polymer chains, and it assumes random mixing. A mixture of two homopolymers and a diblock copolymer is a four-component system, i.e., $n = 3$. We assume incompressibility, and this eliminates correlations with one of the components. This is called the "background" component, and it is labeled 0. We define hPE as the background component; all the multicomponent blends discussed in this paper and in paper II[20] contain hPE. Labels 1 and 2 refer to the PE and PP blocks in the PE−PP block copolymer, respectively, and label 3 refers to the PP homopolymer. Note that components 1, 2, and 3 can be either fully hydrogenated or partially deuterated.

$$B_i = b_i/v_i - b_0/v_0 \qquad (3)$$

where b_i is the scattering length of component i, and v_i is the monomer volume of component i.

The structure factor matrix, $\underline{\underline{S}}(q)$, is given by the solution to the following equation:

$$\underline{\underline{S}}(q) = [\underline{\underline{S}}^0(q)^{-1} + \underline{\underline{V}}(q)]^{-1} \qquad (4)$$

where the elements of $\underline{\underline{S}}^0(q)$ and $\underline{\underline{V}}(q)$ are given by

Table 2. Parameters Used in RPA Calculations at 148 °C

component					hPE−hPP		dPE−dPP	
param	hPE	dPE	hPP	dPP	hPE	hPP	dPE	dPP
N_i[a]	83	83	178	178	367	376	367	376
v_i (Å^3)	179.0	178.8	174.8	174.6	179.0	174.8	178.8	174.6
l_i (Å)	10.79	10.79	8.61	8.61	12.65	10.10	12.65	10.10
b_i (Å) × 10^4	−0.498	4.952	−0.498	5.156	−0.498	−0.498	6.327	3.784

[a] The numbers of monomer units are based on the C_6H_{12} repeat unit. Interaction parameters at 148 °C, based on a reference volume v = 161.5 Å^3, are $\chi_{hPE/dPP} = 1.39 \times 10^{-2}$, $\chi_{dPE/hPP} = 1.03 \times 10^{-2}$; $\chi_{hPE/hPP} = \chi_{dPE/dPP} = 1.39 \times 10^{-2}$; and $\chi_{hPE/dPE} = 6.43 \times 10^{-3}$, $\chi_{hPP/dPP} = 2.66 \times 10^{-4}$. See text for the temperature dependence of these parameters.

$$S^0_{ii}(q) = N_i\phi_i v_i P_i(q) \qquad (i = 1-3) \tag{5}$$

$$S^0_{12}(q) = S^0_{21}(q) = (N_1\phi_1 v_1 N_2\phi_2 v_2)^{1/2} F_1(q)\, F_2(q) \tag{6}$$

$$S^0_{13}(q) = S^0_{23}(q) = S^0_{31}(q) = S^0_{32}(q) = 0 \tag{7}$$

$$V_{ii}(q) = \frac{1}{N_0\phi_0 v_0 P_0(q)} - \frac{2\chi_{i0}}{v} \qquad (i = 1-3) \tag{8}$$

$$V_{ij}(q) = \frac{1}{N_0\phi_0 v_0 P_0(q)} - \frac{\chi_{i0}}{v} - \frac{\chi_{j0}}{v} + \frac{\chi_{ij}}{v} \qquad (\text{all } i \neq j) \tag{9}$$

where ϕ_k is the volume fraction of component k in the blend, N_k is the number of monomers per chain of component k, l_k is its statistical segment length, v_k is the monomer volume, χ_{kl} is the Flory−Huggins interaction parameter between components k and l, and v is a reference volume, which we set equal to 161.5 Å^3. This is the geometric mean of the monomer volumes of (amorphous) PE and PP chains at 23 °C. Function $P_i(q)$ is the Debye function for flexible chains, and $F_i(q)$ is the Leibler function for interblock correlations in a diblock copolymer.

$$P_i(q) = \frac{2}{x_i^2}[\exp(-x_i) + x_i - 1] \tag{10}$$

$$F_i(q) = \frac{1 - \exp(x_i)}{x_i} \tag{11}$$

where $x_i = q^2 R_{g,i}^2 = q^2 N_i l_i^2/6$ and $R_{g,i}$ is the radius of gyration component i.

For binary blends of two homopolymers, eqs 2−11 with $\phi_1 = \phi_2 = 0$ reduce to the de Gennes result,[5]

$$I(q) = \left(\frac{b_0}{v_0} - \frac{b_3}{v_3}\right)^2 \left\{\frac{1}{S^0_{00}} + \frac{1}{S^0_{33}} - \frac{2\chi_{03}}{v}\right\}^{-1} \tag{12}$$

where S^0_{ii} are given by eq 5.

For a pure diblock copolymer melt, eqs 2−11 with $\phi_0 = \phi_3 = 0$ reduce to Leibler's result,[12]

$$I(q) = \left(\frac{b_1}{v_1} - \frac{b_2}{v_2}\right)^2 \left\{\frac{S^0_{11} + S^0_{22} + 2S^0_{12}}{S^0_{11}S^0_{22} - (S^0_{12})^2} - \frac{2\chi_{12}}{v}\right\}^{-1} \tag{13}$$

where S^0_{ii} are given by eq 5 and S^0_{12} is given by eq 6.

Parameter Estimation

The main purpose of this paper is to compute the scattering intensity, $I(q)$, from multicomponent PE/PP/PE−PP blends using eqs 2−11. The parameters that need to be determined are N_i, v_i, l_i, b_i, and χ_{ij} (i, j = 0−3). The values of these parameters are summarized in Table 2. The values of N_i and v_i of all the components were determined from the measured molecular weights and densities. The change in v_i with temperature (d ln v_i/dT) was assumed to be equal to the thermal expansion coefficients of PE and PP, which are 7.4 × 10^{-4} and 7.2 × 10^{-4} 1/K, respectively. The measured PE volume fraction in the PE−PP block copolymer (Table 1) was used to determine N_i of the blocks. The values of b_i for the homopolymers and hPE−hPP were based on the average atomic composition of the components. The other parameters (χ_{ij}, l_i, and b_i for dPE−dPP) were determined from experiments on two-component systems, as described below.

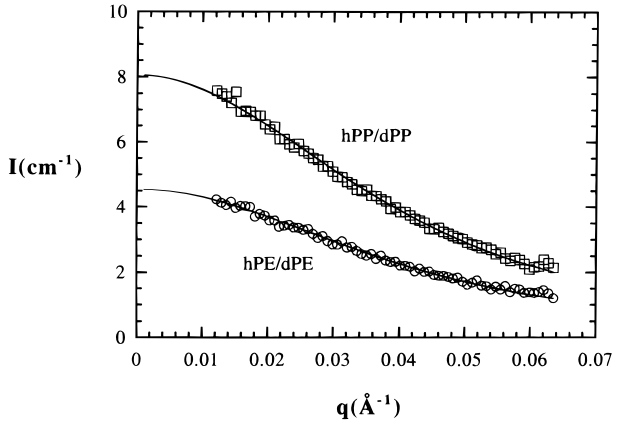

Figure 2. Coherent SANS intensity versus q for matched pair mixtures (hPE/dPE and hPP/dPP) at 148 °C. Solids curves through the data are best fits to eq 12.

1. Scattering from Binary Homopolymer Blends. SANS intensity profiles from a 50/50 mixture of hPE/dPE at 148 °C are represented by circles in Figure 2. We use these data to estimate the statistical segment length of PE chains and to estimate χ between the chains (see refs 29 and 30 for details). The solid curves through the data are least squares RPA fits (eq 12), with l_{PE} ($l_{PE} = l_{hPE} = l_{dPE}$) and $\chi_{hPE/dPE}$ as adjustable parameters. The squares in Figure 2 represent SANS profiles from a 50/50 mixture of hPP/dPP at 148 °C, which give l_{PP} and $\chi_{hPP/dPP}$. The SANS profiles from these blends had a weak temperature dependence in the temperature range of interest (T ranges from 387 to 443 K), indicating a weak temperature dependence of l_i and χ. l_{PE} (Å) = 9.52−0.0044(T−387), l_{PP} (Å) = 7.59−0.0031(T−387), $\chi_{hPE/dPE} = 1.34 \times 10^{-4} + 2.64/T$, and $\chi_{hPP/dPP} = -3.63 \times 10^{-3} + 1.64/T$ (v = 161.5 Å^3). We refer to hPE/dPE and hPP/dPP mixtures as matched pairs.

SANS intensity profiles from binary blends, hPE/dPP and dPE/hPP ($\phi_{PE}/\phi_{PP} = 1.63$ in both cases), at 148 °C are shown in Figure 3. The blend composition is approximately equal to the critical composition for PE and PP chains, based on the Flory−Huggins theory:

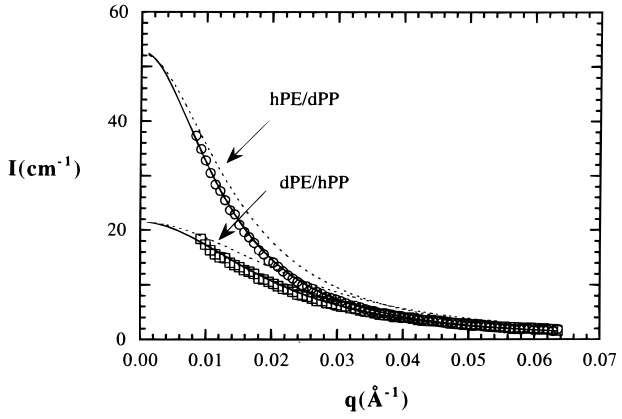

Figure 3. Coherent SANS intensity versus q for critical binary blends, hPE/dPP and dPE/hPP ($\phi_{PE}/\phi_{PP} = 1.63$), at 148 °C. Solid curves through the data are best fits to eq 12 using χ and α as adjustable parameters. The dashed curves are best fits to eq 12 using χ as the only adjustable parameter and the matched pair results for l_{PE} and l_{PP}.

$$\phi_{PE} = \frac{1}{1 + (N_{PE}v_{PE}/N_{PP}v_{PP})^{1/2}} \quad \text{at the critical point} \tag{14}$$

The dashed curves in Figure 3 are RPA fits (eq 12) with χ as the adjustable parameter and matched pair values for l_{PE} and l_{PP}. In principle, the statistical segment lengths of PE and PP chains should be independent of blend composition and therefore matched pair values of l_{PE} and l_{PP} should be applicable to PE/PP blends. However, we find that the measured SANS profiles from the critical PE/PP blends are inconsistent with the matched pair values of l_{PE} and l_{PP}; compare dashed curves with experimental data in Figure 3. Both l_{PE} and l_{PP} were multiplied by a constant, α, so that

$$l_{PE} = \alpha l_{PE,m};\ l_{PP} = \alpha l_{PP,m} \tag{15}$$

where $l_{i,m}$ indicates the matched pair result. The solid curves through the data in Figure 3 are the results of nonlinear regression with χ and α as adjustable parameters. It is evident that the agreement between theory and experiment is much better after the α adjustments are made. The values of α required to force agreement between theory and experiments were α(hPE/dPP) = 1.15 and α(dPE/hPP) = 1.25.

The temperature dependence of the SANS profiles from hPE/dPP blends along with RPA fits are shown in Figure 4. These data enable us to determine the temperature dependence of $\chi_{hPE/dPP}$. Similar measurements were made on dPE/hPP blends to determine the temperature dependence of $\chi_{dPE/hPP}$. The values of α in both blends (hPE/dPP and dPE/hPP) were independent of temperature. Figure 5 shows the measured temperature dependence of the χ parameters ($v = 161.5$ Å^3), which can be approximated by the following equations.

$$\chi_{hPE/dPP} = 17.56/T - 2.76 \times 10^{-2} \tag{16}$$

$$\chi_{dPE/hPP} = 17.60/T - 3.11 \times 10^{-2} \tag{17}$$

It is evident from eqs 16 and 17 and Figure 5 that the main effect of switching the deuterium labels from one component to the other is to induce a vertical shift in the χ versus $1/T$ plots. This is in agreement with

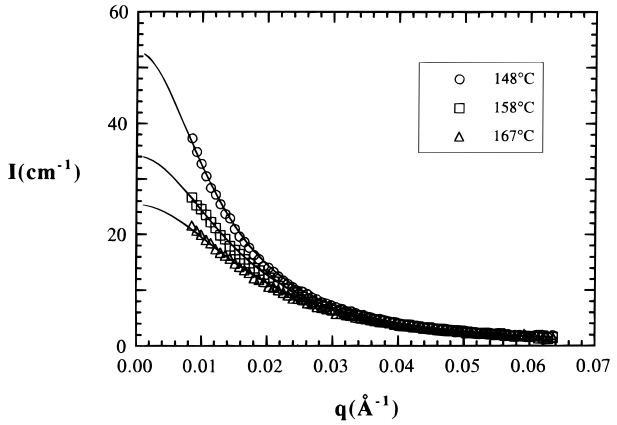

Figure 4. Coherent SANS intensity versus q for the critical hPE/dPP blend ($\phi_{PE}/\phi_{PP} = 1.63$) at selected temperatures. The solid curves through the data represent eq 12 with χ and α as adjustable parameters.

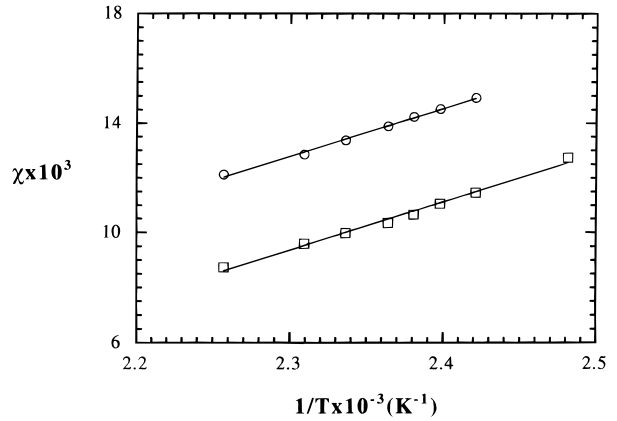

Figure 5. Temperature dependence of Flory−Huggins interaction parameters for critical binary PE/PP blends ($\phi_{PE}/\phi_{PP} = 1.63$): hPE/dPP (circles); dPE/hPP (squares).

previous thermodynamic studies on mixtures of labeled and unlabeled polyolefins.[42,43]

The critical temperature (T_c) of binary homopolymer blends can be estimated on the basis of the Flory−Huggins theory:

$$\chi = \frac{v}{2}\left\{\frac{1}{(N_{PE}v_{PE})^{1/2}} + \frac{1}{(N_{PP}v_{PP})^{1/2}}\right\}^2 \quad \text{at the critical point} \tag{18}$$

Substituting values of N_i and v_i, we get χ (at the critical point) $= 1.57 \times 10^{-2}$ for PE/PP blends. From eq 16 we get T_c(hPE/dPP) = 133 °C. Small angle light-scattering experiments were performed to confirm the location of the critical point. In Figure 6 we show the time dependence of the scattered intensity at low angles after quenching the hPE/dPP blend from 160 °C to a series of temperatures. An increase in the scattered light is detected when the quench temperature was ≤140 °C. On the other hand, no change was recorded when the quench temperature was ≥145 °C. This indicates that the macrophase transition temperature in the hPE/dPP blend is 142.5 ± 2.5 °C. The absolute critical temperatures determined from light and neutron scattering for the hPE/dPP blend are in reasonable agreement (within 2%).

We performed similar experiments on the dPE/hPP blend. There was no detectable change in the light-scattering intensity when this blend was quenched to

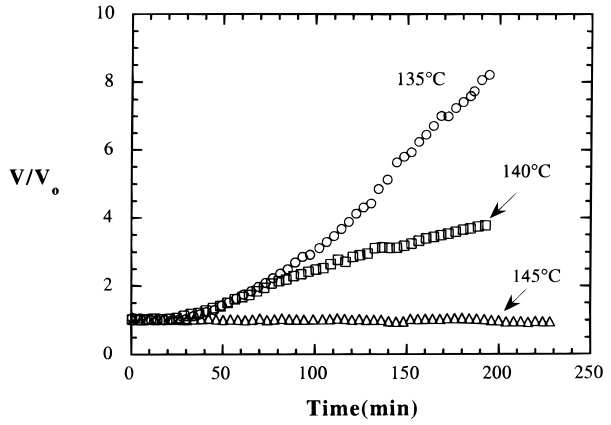

Figure 6. Time dependence of the normalized light-scattering intensity from the critical hPE/dPP blend after the sample was quenched from 160 °C to several temperatures, as indicated. V is the signal from the photodetector, and V_0 is the signal at $t = 0$. Evidence for macrophase separation is seen at temperatures ≤140 °C.

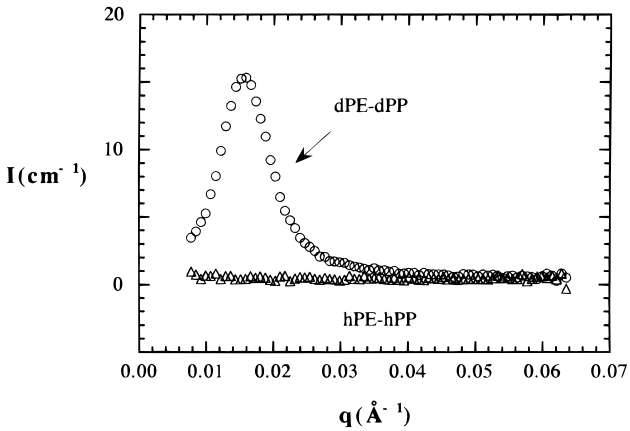

Figure 7. Coherent SANS intensity versus q obtained from pure hPE−hPP and dPE−dPP block copolymers at 167 °C.

temperatures ranging from 150 to 130 °C, which is the temperature range over which the neutron scattering experiments were conducted. This indicates that the onset of macrophase separation occurs at temperatures below 130 °C, and this is consistent with neutron-scattering results (Figure 5). We performed similar light-scattering experiments on hPE/hPP and dPE/dPP blends with $\phi_{PE}/\phi_{PP} = 1.63$. Both blends exhibited macrophase separation at temperatures below 140 °C and single-phase characteristics at temperatures above. This implies that the critical temperature of hPE/dPP, hPE/hPP, and dPE/dPP blends are within experimental error. In other words, at 142.5 °C, the χ parameter in these three blends is equal to 1.57×10^{-2}. It is not possible to measure the χ parameter at other temperatures in hPE/hPP and dPE/dPP blends by SANS due to a lack of neutron scattering contrast between the components. If we assume that deuterium substitution can only induce a vertical shift in the χ versus $1/T$ plot (this assumption is consistent with all published data of mixtures of deuterated and hydrogenous polyolefins), then we are led to the conclusion that χ in hPE/dPP, hPE/hPP, and dPE/dPP blends are identical to each other at all temperatures and are given by eq 16 while χ in dPE/hPP blends is lower by an amount $\Delta\chi$, which is given by the difference between the right-hand sides of eqs 16 and 17.

Some aspects of the effect of deuterium substitution on PE/PP blends is in agreement with previous studies[42,43] while others are not. In this work we find that χ(hPE/dPP) > χ(dPE/hPP) and that the χ versus $1/T$ plots for these two systems are parallel to each other. These results are in agreement with the results presented in refs 42 and 43. On the other hand, our results regarding the location of the critical temperature in hPP/hPE and dPP/dPE blends are not in agreement with results presented in refs 42 and 43. In these studies it was found that the critical temperature of the unlabeled blends was equal to the arithmetic average of the critical temperatures of the singly labeled blends. It is evident that the effect of deuterium labeling on thermodynamics is not completely understood.

2. Determination of Deuterium Content in the dPE−dPP Block Copolymer. The SANS data from hydrogenated and deuterated PE−PP block copolymers at 167 °C are shown in Figure 7. The scattering intensity from hydrogenated PE−PP is very low and q-independent. This is expected because the neutron-scattering contrast between the hPE and the hPP blocks is negligible. In contrast, the scattering intensity from deuterated PE−PP has a peak at $q = 0.016$ Å^{-1}. The presence of a scattering peak indicates a substantial difference in the average scattering lengths (b_i) of PE and PP blocks of the dPE−dPP copolymer (the monomer volumes, v_i, are nearly identical). To estimate the average scattering lengths of the two blocks we need two equations, i.e., two measurements. The SANS profile from dPE−dPP at 167 °C, and the ratio of the densities of dPE−dPP and hPE−hPP at 23 °C, are the two measurements used here.

Let x be the average number of deuterium atoms per monomer for the PE block and y be the average number of deuterium atoms per monomer for the PP block. The chemical formulas for the monomers are $C_6H_{12-x}D_x$ (PE) and $C_6H_{12-y}D_y$ (PP). Based on the known scattering lengths of the constituent atoms, the scattering lengths of the PE and PP monomers can be written as

$$b_{PE}\,(\text{cm}) = -0.498 \times 10^{-12} + 1.014 \times 10^{-12}x \quad (19)$$

$$b_{PP}\,(\text{cm}) = -0.498 \times 10^{-12} + 1.014 \times 10^{-12}y \quad (20)$$

In this section, the subscripts PE and PP refer to the blocks in the dPE−dPP copolymer. The structure factor of the block copolymer, $S(q)$, defined as

$$S(q) = \frac{I(q)}{\left(\frac{b_{PE}}{v_{PE}} - \frac{b_{PP}}{v_{PP}}\right)^2} \quad (21)$$

can, in principle, be estimated from the measured χ and l_i obtained from the SANS measurements on binary blends. However, the q value at the scattering peak, q_{peak}, from dPE−dPP indicates that the l_i values in the block copolymer are about 25% larger than those obtained from the binary blends. In addition, it is not certain that χ measured in binary blends is applicable to block copolymer melts. To circumvent these difficulties, we focus on the scattering data at high q in the Kratky regime. In the limit of high q, the product $S(q)q^2$ becomes independent of χ (also called the Kratky plateau) and is given by

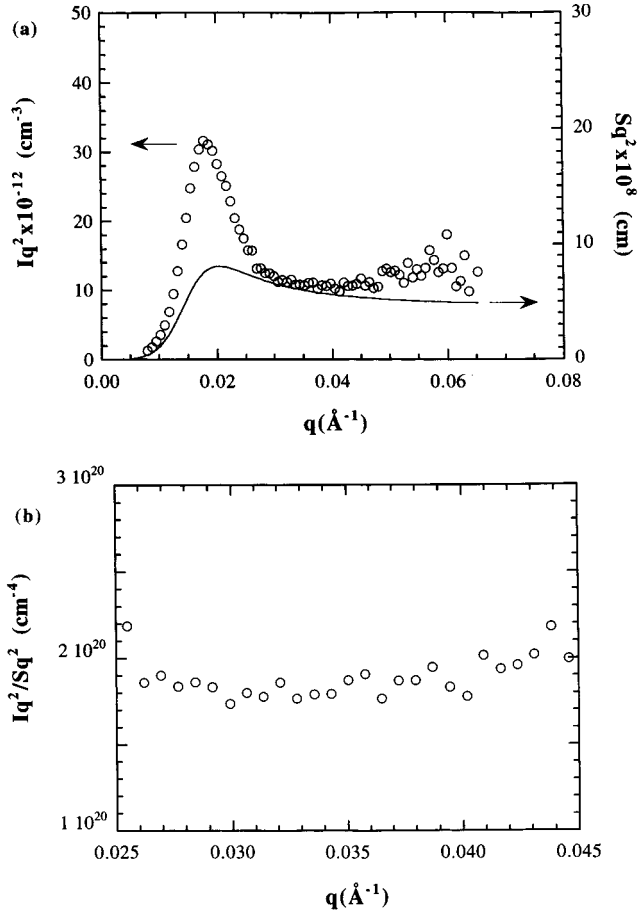

Figure 8. (a) Kratky plots obtained from the experimental SANS data from dPE−dPP (Iq^2) and the RPA predictions (Sq^2) (b) The contrast factor Iq^2/Sq^2, obtained from the data shown in Figure 8a, is plotted versus q in the high-q range.

$$Sq^2 = 12\left\{\frac{N_{PE}\phi_{PE}v_{PE}N_{PP}\phi_{PP}v_{PP}}{N_{PE}{}^2\phi_{PE}v_{PE}l_{PE}{}^2 + N_{PP}{}^2\phi_{PP}v_{PP}l_{PP}{}^2}\right\}$$
for pure block copolymers only (22)

We estimated the scattering contrast between the blocks by comparing the measured $I(q)q^2$ with RPA calculations of $S(q)q^2$, as shown in Figure 8 (a). The ratio $I(q)q^2/S(q)q^2$ in the high-q regime is shown in Figure 8b. For completeness, we used the full expression for $S(q)$ with the binary blend χ parameter, rather than eq 22. The average value of this ratio gives an estimate of the scattering contrast in dPE−dPP:

$$\left(\frac{b_{PE}}{v_{PE}} - \frac{b_{PP}}{v_{PP}}\right)^2 = \left\{\frac{I(q)q^2}{S(q)q^2}\right\}_{\text{at high } q} = 1.798 \times 10^{20}\ \text{cm}^{-4} \quad (23)$$

Equations 19, 20, and 23 give us one relationship between x and y.

The ratio of the measured densities of hPE−hPP and dPE−dPP at 23 °C (see Table 1) gives another relationship between x and y:

$$\frac{N_{PE}(84.16 + x) + N_{PP}(84.16 + y)}{84.16(N_{PE} + N_{PP})} = \frac{\rho_{dPE-dPP}}{\rho_{hPE-hPP}} = 1.0561 \quad (24)$$

Simultaneous solution of eqs 19, 20, 23, and 24 give $x = 5.98$ and $y = 3.49$.

3. Order to Disorder Transition in the dPE−dPP Block Copolymer. Pioneering experiments by Bates et al. demonstrated that a clear signature of the order to disorder transition (ODT) in block copolymer melts can be obtained if a bias is introduced in the alignment of the ordered phase.[44] This leads to anisotropic scattering profiles, and the ODT can be identified as the point at which the scattering profiles lose their asymmetry. In symmetric block copolymers such as dPE−dPP, the ordered phase is undoubtedly lamellar. We gently tapped the brass housing within which the sample was held, while it was at 120 °C. We found that this perturbation produced an azimuthally asymmetric SANS profile, indicating a nonrandom distribution of lamellar orientation. The sample was then heated quiescently in steps of 3 °C. The neutron scattering profiles along the vertical and horizontal directions of the 2-dimensional detector are shown at selected temperatures in Figure 9. Anisotropic scattering patterns were found at temperatures ≤148 °C. When the sample was heated to 151 °C, the scattering anisotropy disappeared abruptly. The scattering pattern at temperatures ≥151 °C remained isotropic.

In Figure 10, we plot the temperature dependence of ΔI, the difference of the peak intensity in the vertical and horizontal directions. The ODT, which occurs at 149.5 ± 1.5 °C, is identified by a discontinuous decrease in ΔI to values that are in the vicinity of zero. The discontinuity is expected due to the weakly first-order nature of the ODT.[12,42]

SANS experiments were also performed on an unperturbed dPE−dPP sample, which yielded isotropic scattering patterns at all temperatures. It is well-known that the ODT is accompanied by an abrupt broadening of the SANS peak.[45−47] The broadening can be identified by estimating the width (σ) of the scattering peak as a function of temperature. We fit the experimental data in the vicinity of the peak to a Gaussian function to obtain σ; $I(q) = I_0 \exp\{-2(q - q_{peak})^2/\sigma^2\}$, where I_0 and q_{peak} are the peak height and position, respectively. In Figure 11, we plot the temperature dependence of σ. An abrupt break in the σ versus T plot is evident at 149 °C, signifying an ODT. The location of the ODT estimated from the temperature dependence of σ and that of ΔI are in good agreement.

4. Estimation of χ and l_i in the dPE−dPP Block Copolymer. We fit the measured SANS profiles above 149 °C to the RPA predictions (eq 13), with χ and α as adjustable parameters. The results are shown in Figure 12. The agreement between theory and experiment is reasonable. The experimental scattering peaks are broader than the theoretical scattering curves. This effect, which is most noticeable near the ODT (151 °C), was also observed in our previous study of scattering from block copolymer melts.[33] In that study we showed that the observed broadening was due to instrumental smearing. However, the difference between the values of χ and l_i obtained after correcting for instrumental smearing and those obtained without correcting for this effect was less than 1%. We also studied the effect of chain polydispersity of our estimates of χ and l_i. This effect is most pronounced near the ordering transition. The value of χ at 151 °C, after correcting for a polydispersity index of 1.12, was 11.4×10^{-3}, which is close to the uncorrected value of 12.6×10^{-3} ($v = 161.5$ Å^3). Since the effect of instrumental smearing and component polydispersity is not large, we ignore these correc-

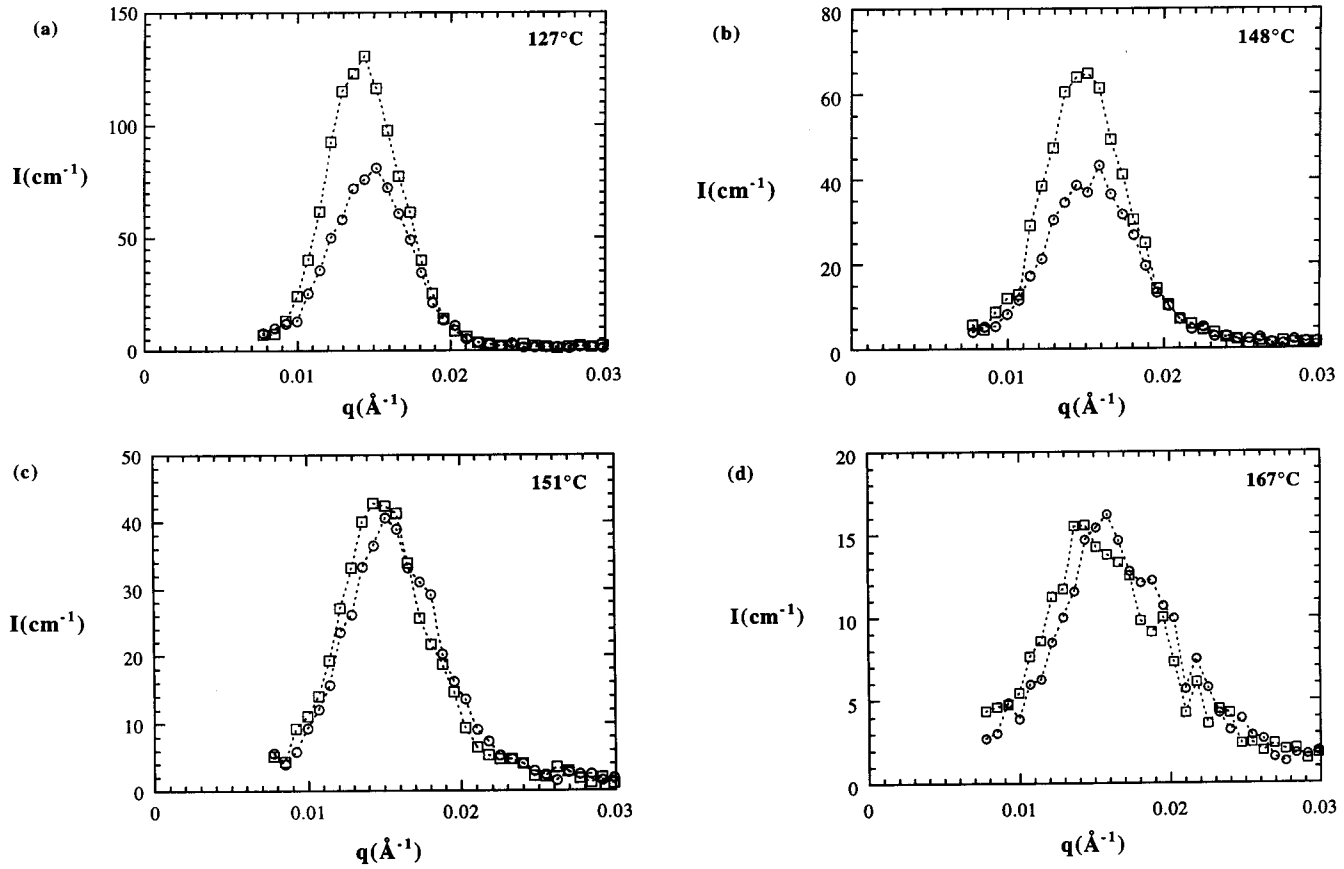

Figure 9. Coherent SANS intensity profiles in the vertical (squares) and horizontal (circles) directions of the two-dimensional detector, for pure dPE−dPP after perturbation (see text for details): anisotropic scattering patterns at (a) 127 °C and (b) 148 °C; isotropic scattering patterns at (c) 151 °C and (d) 167 °C.

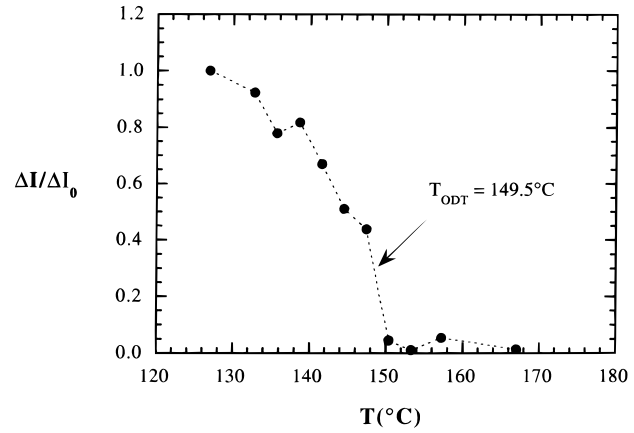

Figure 10. Temperature dependence of the $\Delta I/\Delta I_0$ obtained from SANS experiments on pure dPE−dPP after the sample was perturbed (see text). The difference of scattered intensity in the vertical and horizontal directions is ΔI. ΔI_0 is ΔI at 127 °C.

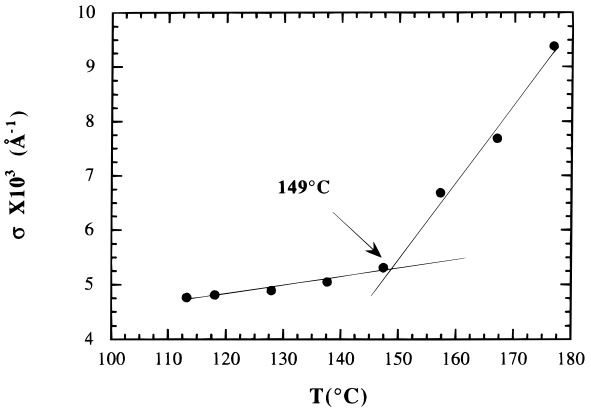

Figure 11. Temperature dependence of the average peak width (σ) obtained from SANS experiments on pure dPE−dPP without perturbations. The lines are linear fits through the high- and low-temperature data.

tions in the remainder of this paper and in paper II. It should be noted that accounting for polydispersity and instrumental smearing in multicomponent blends will require a substantial extension of the current theoretical approach.

In Figure 13, we compare the χ parameter between unlabeled PE and PP chains, $\chi_{PE/PP}$, obtained by fitting binary blend SANS data (hatched squares) with that from the dPE−dPP block copolymer (circles). The deviations between these two sets of data are 10% or less. Fredrickson and Helfand have shown that concentration fluctuations lead to non-mean-field effects, which affect the measurement of χ.[48] The χ parameter obtained after fluctuation corrections (see ref 33 for details) are also shown in Figure 13. It is evident that the χ parameter obtained from the homopolymer blends and that obtained from the block copolymer after fluctuation corrections are in surprisingly good agreement.

This completes the characterization of all the components used in this study, and the results are summarized in Table 2. Estimates of the radii of gyration of the polymer chains used in this study are summarized in Table 3.

The measured χ parameters from dPE−dPP are consistent with data published by Rangarajan et al.,[49]

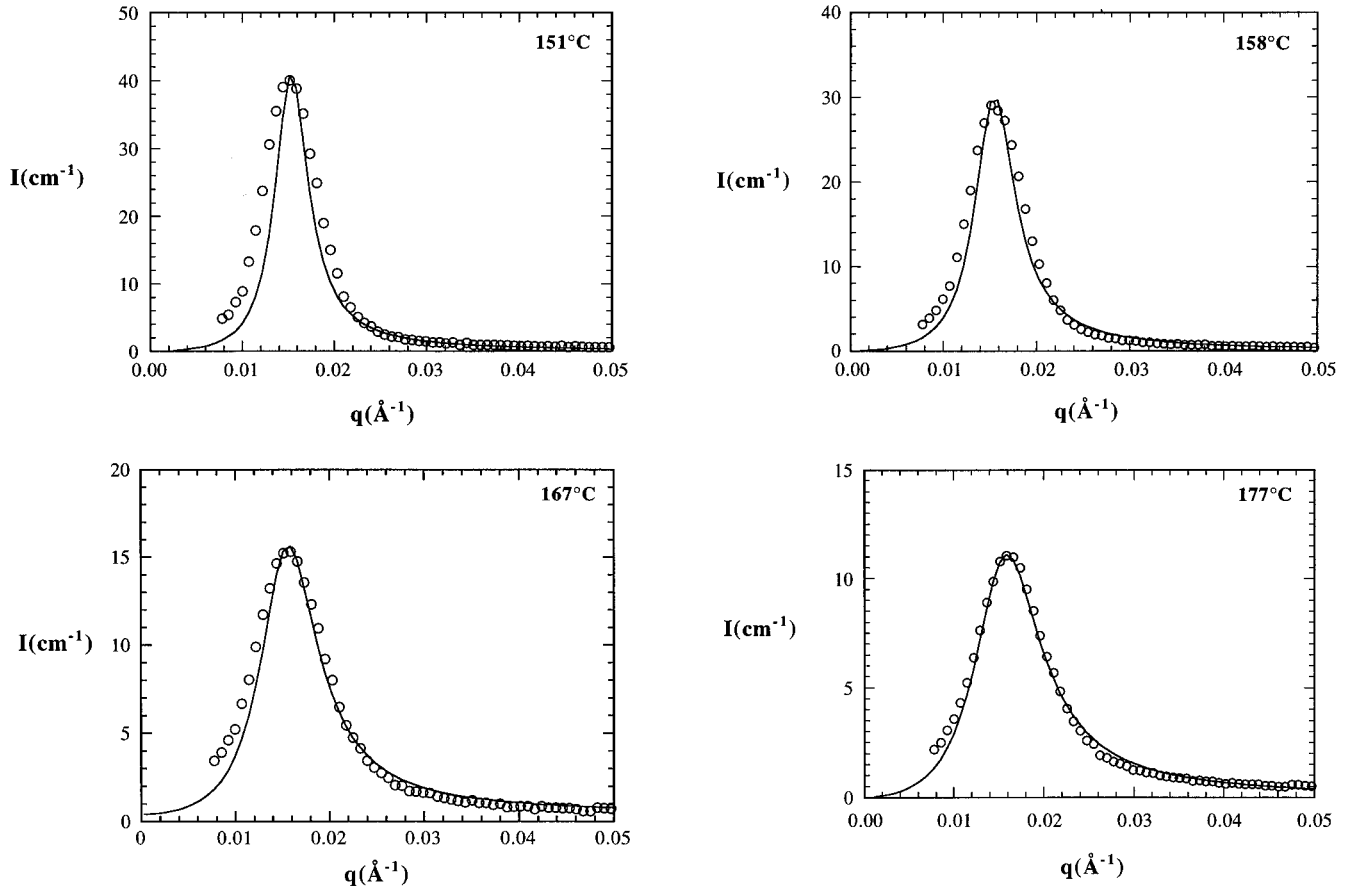

Figure 12. Comparison of measured SANS intensity profiles and RPA-based theory, for a disordered melt of dPE−dPP, using χ and α as adjustable parameters.

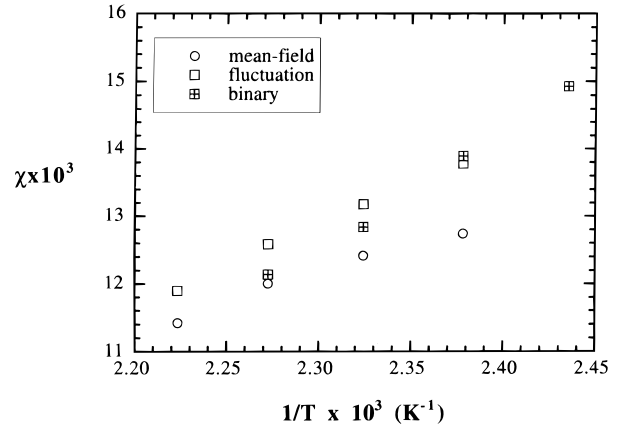

Figure 13. Temperature dependence of the Flory−Huggins interaction parameter between unlabeled PE and PP chains, χ, based on measurements on binary PE/PP blends (hatched squares), and the dPE−dPP block copolymer. The data obtained from the block copolymer were analyzed using RPA-based mean-field theory (circles) and fluctuation corrections proposed by Fredrickson and Helfand (open squares).

who located the ODT of a PE−PP block copolymer by noting the temperature at which the rheological properties of the material changed abruptly. This result of Rangarajan et al. was very valuable because the target molecular weights of the components that were chosen for this study were based on it.

Predicted SANS Profiles from Multicomponent PE/PP/PE−PP Blends

We are now in a position to calculate the scattering profiles from single-phase, multicomponent blends composed of PE, PP, and PE−PP. The calculations presented here are based on statistical segment lengths given in Table 2, and χ parameters obtained from binary blends. We restrict our attention to hPE/dPP/hPE−hPP mixtures. These profiles reflect the arrangement of the dPP chains, since the scattering contrast between the other three components is negligible. The calculations are restricted to blends with $\phi_{PE}/\phi_{PP} \approx 1.63$ and block copolymer volume fractions ranging from 0.05 to 0.75. The exact compositions used in these calculations are given in Table 4, and they correspond to the composition of the blends on which the experiments reported in

Table 3. Estimates of Molecular Dimensions

	R_g (Å) based on statistical segment lengths from SANS on		
polymer	matched pairs	PE/PP blends	PE−PP block copolymer
hPE, dPE	35	40	
hPP, dPP	41	45	
hPE−hPP, dPE−dPP	95	107	126

Table 4. Composition of the Multicomponent Blends Examined

blend designation	components			compositions	
	A	B	A−B	ϕ_A/ϕ_B (ϕ_A)	ϕ_{A-B}
BH05	hPE	dPP	hPE−hPP	1.6298 (0.5890)	0.0496
BH10	hPE	dPP	hPE−hPP	1.6379 (0.5588)	0.1001
BH15	hPE	dPP	hPE−hPP	1.6306 (0.5275)	0.1489
BH20	hPE	dPP	hPE−hPP	1.6191 (0.4948)	0.1996
BH30	hPE	dPP	hPE−hPP	1.6256 (0.4334)	0.3000
BH50	hPE	dPP	hPE−hPP	1.6188 (0.3055)	0.4946
BH75	hPE	dPP	hPE−hPP	1.6188 (0.1554)	0.7486

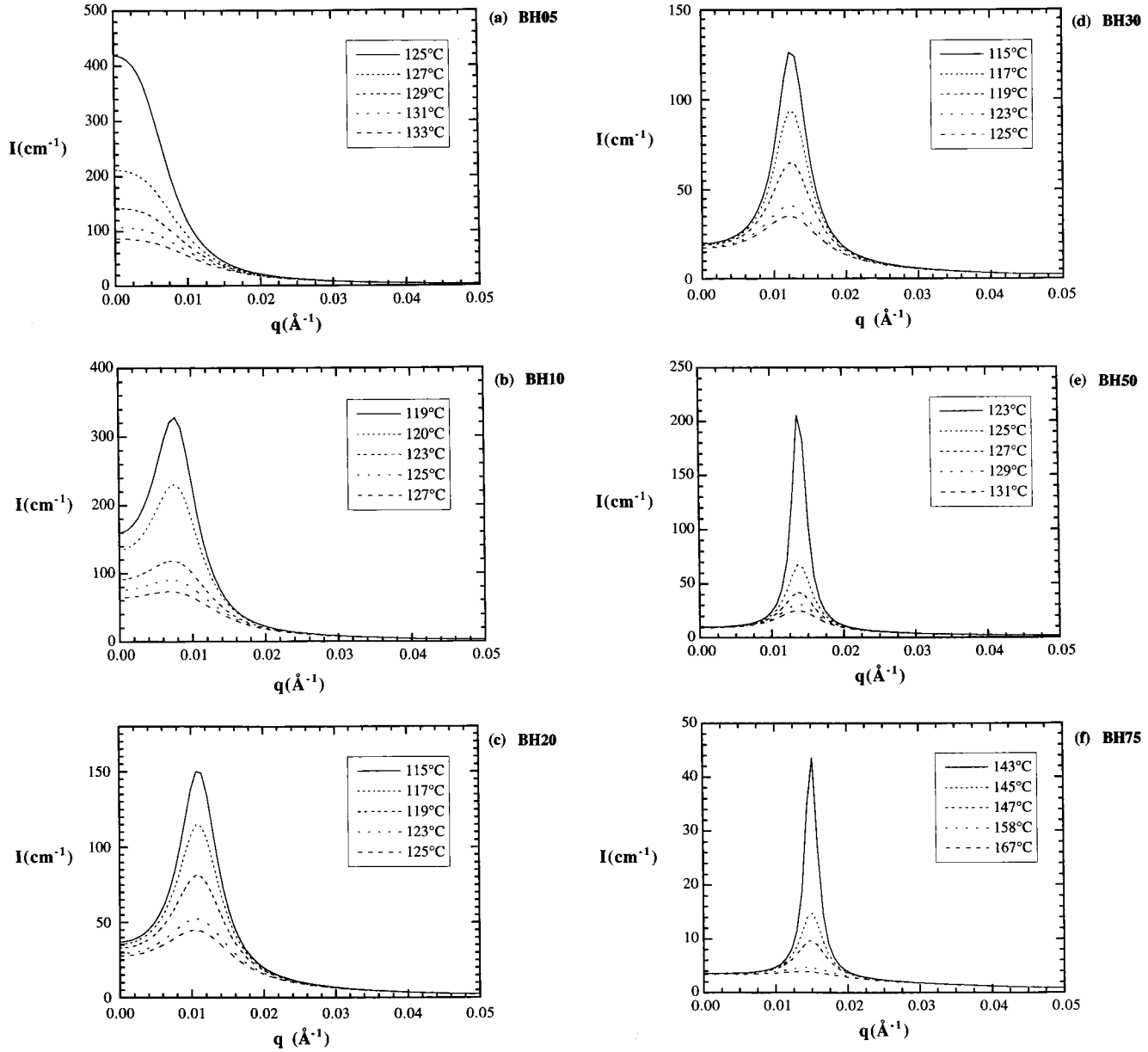

Figure 14. Predicted SANS intensity versus q of ternary hPE/dPP/hPE−hPP blends based on RPA at various block copolymer concentrations and temperatures: (a) blend BH05 (5% block copolymer); (b) BH10; (c) BH20; (d) BH30; (e) BH50; (f) BH75.

paper II[20] were performed. The blends are labeled BH*ij*, where *ij* is the volume percent of block copolymer.

We use the calculated scattering profiles to construct a phase diagram for these PE/PP/PE−PP blends, using the following assumptions: (1) If the calculated scattering profiles in the vicinity of the phase transition temperature are monotonic functions of q (i.e., no peaks at finite q), then we assume that the system exhibits macrophase separation. (2) If the calculated scattering profiles in the vicinity of the phase transition temperature have a scattering peak at finite scattering angles, then we assume that the system exhibits microphase separation. In simple block copolymer melts, the periodicity of the ordered phases formed in the vicinity of the order-to-disorder transition is nearly identical to the characteristic length of the concentration fluctuations in the disordered state. The size of the microphases is thus roughly given by $2\pi/q_{peak}$.

Selected scattering profiles obtained by using multicomponent RPA (eqs 2−11) are shown in Figure 14. In Figure 14a, we show calculated SANS profiles for blend BH05, which contains 5% block copolymer, at temperatures ≥125 °C. The scattering profiles are monotonic functions of q at all temperatures. The calculated scattering intensities at 123 °C are negative at some q values, implying a breakdown of the RPA. This indicates that a phase boundary has been crossed between 125 and 123 °C. We conclude that this blend will exhibit a macrophase separation transition at 124 ± 1 °C, on the basis of the criteria described in the beginning of this section.

In Figure 14b, we show the scattering intensity profiles for BH10 with 10% block copolymer. The scattering profiles at temperatures above 127 °C do not have scattering peaks and are qualitatively similar to those obtained from sample BH05. However, at lower temperatures, we see a scattering peak at $q = 0.0078$ Å^{-1}. The peak becomes more pronounced with decreasing temperature. The computed scattering intensities at 115 °C were negative at some q values, indicating the occurrence of a phase transition at 116 ± 1 °C. We conclude that this blend will exhibit microphase separa-

tion, on the basis of the criteria described earlier in this section. However, the estimated periodicity of the "microphases" is 800 Å ($2\pi/q_{peak}$), which is large compared to typical microphases found in block copolymers.[10−12,33,44−47] In addition, there is a large increase in the low-angle scattering ($q < q_{peak}$) at low temperatures, indicating the presence of large-length-scale structures. It is evident that the microphases in BH10 bear some similarity with conventional macrophases. In these multicomponent blends, the distinction between microphases and macrophases is no longer as clear as it was in the case of two-component systems such as binary homopolymer blends and block copolymers. This is characteristic of systems in the vicinity of the Lifshitz line.[14,24,27,28]

In Figure 14c,d, we show SANS profiles for BH20 and BH30, containing 20% and 30% block copolymer, respectively, in the single-phase region. These scattering profiles are qualitatively similar to those obtained for BH10. Decreasing temperature leads to the development of a scattering peak, as well as an increase in the forward scattering. The microphase transition temperature for BH20 and BH30 is 112 ± 1 °C. The scattering peaks in BH20 and BH30 appear at $q = 0.011$ Å^{-1} and $q = 0.013$ Å^{-1}, respectively. This indicates that the periodicity of the ordered phases in BH20 and BH30 is 570 and 480 Å, respectively. In a conventional symmetric block copolymer, the characteristic length of the ordered phase is $d = (2\pi/1.946)R_g$, which gives 407 Å for the pure PE−PP block copolymer.[12] The ordered phases formed in BH20 and BH30 may therefore be regarded as swollen, block copolymer microphases. Note, however, that we are studying the arrangement of the dPP chains, which have an R_g of 45 Å (see Table 3). We thus see a periodic clustering of the homopolymer chains, with the PE−PP block copolymer serving as the invisible scaffolding.

In Figure 14e,f, we show calculated intensity profiles for BH50 and BH75. The concentration fluctuations in these blends are similar to that in pure block copolymers. The scattering intensity in the forward direction is small (but nonzero) and a weak function of temperature. Using the criteria described above, we conclude that the microphase transition temperatures for BH50 and BH75 are 122 ± 1 and 142 ± 1 °C, respectively.

The phase diagram for hPE/dPP/hPE−hPP blends is shown in Figure 15. The solid curve represents the border between single-phase systems at high temperatures and phase-separated systems at low temperatures. The open circles represent liquid−liquid phase transition points, i.e., the formation of macrophases. The filled symbols represent the order−disorder phase transition points, i.e., the formation of periodic microphases. The solid vertical line is a boundary between macrophase-separated and microphase-separated states. The vertical dashed line represents the boundary between homogeneous, liquidlike phases with a scattering peak at $q = 0$ and homogeneous, disordered phases with a peak at finite q. The symbol L represents homogeneous, liquidlike systems, while the symbol D represents homogeneous, disordered systems. The symbol M represents the phase-separated state with macrophase separation. The symbol O represents the ordered state obtained due to microphase separation. The crystalline melting temperature for the pure components is in the vicinity of 110 °C. The crystalline phases are not of interest and therefore not shown in Figure 15.

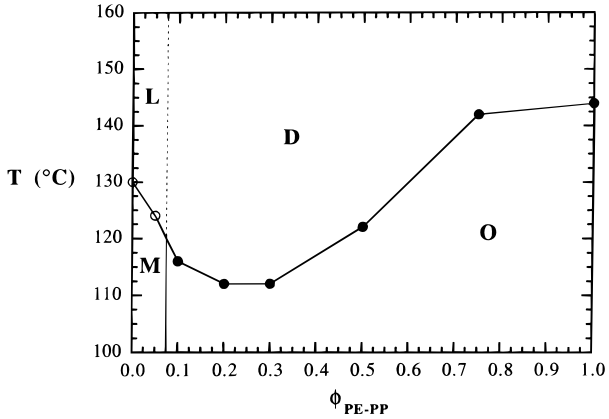

Figure 15. Phase diagram for hPE/dPP/hPE−hPP blends with $\phi_{PE}/\phi_{PP} \approx 1.63$, based on RPA calculations. The circles represent phase transition points: macrophase transitions (open circles) and microphase transitions (filled circles). In region L, the calculated scattering profiles are liquidlike and contain no peaks, and these systems are assumed to form macrophases (M) at low temperatures. In region D, the calculated scattering profiles contain peaks (i.e. disordered systems), and these systems are assumed to form ordered microphases (O) at low temperatures.

Concluding Remarks

In this paper we have studied the thermodynamic properties of PE/PP/PE−PP blends. Neutron and light scattering experiments were conducted on critical, binary PE/PP ($\phi_{PE}/\phi_{PP} = 1.63$) blends and a symmetric PE−PP block copolymer. The binary blend exhibited a liquid−liquid phase transition at 143 °C, while the block copolymer exhibited an order−disorder transition at 149 °C. We fit the neutron scattering profiles from these simple systems in the single-phase regime to theoretical predictions based on the RPA, to obtain estimates of the Flory−Huggins interaction parameter and the statistical segment lengths. The χ parameter measured in binary PE/PP blends and the PE−PP block copolymer were not in quantitative agreement, indicating a breakdown of the mean-field theory. Accounting for fluctuation effects brings the χ determined in the block copolymer in close agreement with that measured in the binary homopolymer blends.

The scattering profiles of a series of multicomponent PE/PP/PE−PP blends with $\phi_{PE}/\phi_{PP} \approx 1.63$ were then computed, using multicomponent random phase approximation. The computed scattering curves from BH05 (with 5% block copolymer), in the vicinity of the phase transition point, indicated that this blend would undergo macrophase separation. On the other hand, blends in which the volume fraction of the block copolymer was greater than or equal to 10% exhibited scattering peaks, which were assumed to be announcements of microphase separation. However, the distinction between order and disorder was quite subtle. The onset of a phase transition is characterized by a divergence in scattering intensity, either at $q = 0$, or at finite q. In blend BH10, we find that the intensity at both $q = 0$ and $q = q_{peak} = 0.0078$ Å^{-1} increase rapidly as the phase transition temperature is approached. In Figure 16 we plot $1/I(q = q_{peak})$ and $1/I(q = 0)$ versus $1/T$ for BH10. The temperature at which $1/I(q = 0) \rightarrow 0$ is 114 °C, while the temperature at which $1/I(q = q_{peak}) \rightarrow 0$ is 117 °C. These temperatures are very close to each other, and therefore this system is delicately placed at the border between microphase and macrophase

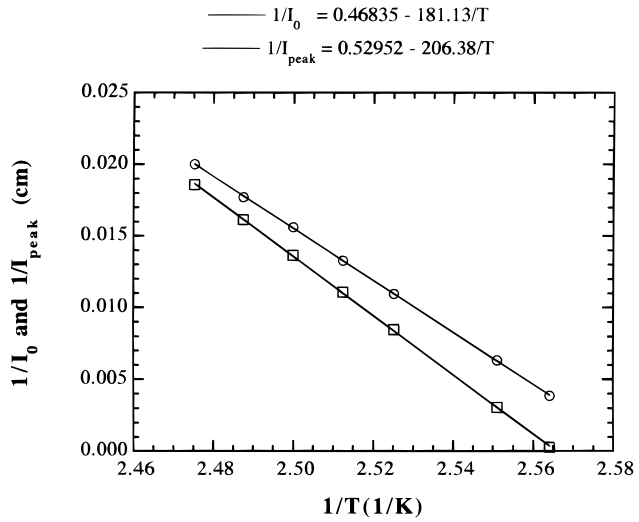

Figure 16. Calculated values of $1/I(q = q_{peak})$ (squares) and $1/I(q = 0)$ (circles) versus $1/T$ for BH10 (10% block copolymer) based on the RPA.

separation, i.e., near the Lifshtiz line. It is possible that mean-field theories break down in this regime. In addition, the computed scattering curves for BH10 are sensitive to small changes in the parameters, particularly, N_i and χ_{ij}. We must therefore treat the predictions of multicomponent RPA in the vicinity of $\phi_{PE-PP} = 0.1$ with extreme caution.

In paper II, which follows this paper, we compare the theoretical predictions presented here with experimental data from PE/PP/PE−PP blends.

Acknowledgment. Financial support from the National Science Foundation to Polytechnic University (DMR-9457950), the 3M Non-Tenured Faculty Award, and the Exxon Education Foundation is gratefully acknowledged. We thank the scientists at the National Institute of Standards and Technology[50] for their help with the SANS measurements. We thank Alessandro Faldi, Dave Lohse, Pratima Rangarajan, Glenn Reichart, and Charles Ruff for their help in characterizing the polyolefins, and the reviewers for their constructive criticism and valuable suggestions.

References and Notes

(1) Paul, D. R., Newman, S., Eds, *Polymer Blends*; Academic Press: New York, 1978.
(2) Dutta, S.; Lohse, D. J. *Polymeric Compatibilizers*; Hanser: Cincinnati, OH 1996.
(3) (a) Unpublished lectures by M. Tirrell. (b) de Gennes, P. G.; Badoz, J. *Fragile Objects*; Springer-Verlag: New York, 1996.
(4) Most of the reported studies on homogeneous polymer blends have used neutron scattering. In principle, other sources such as light can be used, as demonstrated in ref 7.
(5) de Gennes, P. G. *Scaling Concepts in Polymer Physics*; Cornell University Press: Ithaca, NY, 1979.
(6) Higgins, J. S.; Benoit, H. C. *Polymers and Neutron Scattering*; Oxford: New York, 1994.
(7) Meier, G.; Momper, B.; Fischer, E. W. *J. Chem. Phys.* **1992**, 97, 5884.
(8) The characteristics of liquid−liquid phase separation are summarized in ref 9. In the early stages of phase separation, uniform phase sizes (i.e., a periodic structure) emerge if spinodal decomposition is the mechanism of phase separation. However, this uniformity is lost as coarsening continues and the system approaches equilibrium. During nucleation and growth, a wide distribution of phase sizes is expected during all stages of phase separation.
(9) Gunton, J. D.; San Miguel, M.; Sahani, P. S. *Phase Transitions*; Academic Press: New York, 1983; Vol. 8.
(10) Roe, R. J.; Fishkis, M.; Chang, J. C. *Macromolecules* **1981**, *14*, 1091.
(11) Hashimoto, T.; Shibayama, M.; Kawai, H. *Macromolecules* **1983**, *16*, 1093.
(12) Leibler, L. *Macromolecules* **1980**, *13*, 1602.
(13) Allen, S. M.; Thomas, E. L. *The Structure of Materials*; Wiley: New York, 1997.
(14) Chakin, P. M.; Lubensky, T. C. *Principles of Condensed Matter Physics*; Cambridge: New York, 1995.
(15) Benoit, H.; Benmouna, M.; Wu, W. L. *Macromolecules* **1990**, *23*, 1511.
(16) Akcasu, A. Z.; Tombakoglu, M. *Macromolecules* **1990**, *23*, 607.
(17) Akcasu, A. Z.; Klein, R.; Hammouda, B. *Macromolecules* **1993**, *26*, 4136.
(18) Balsara, N. P. In *Physical Properties of Polymers Handbook*; AIP Press: Woodbury, New York, 1996; Chapter 19, p 257.
(19) Fetters, L. J.; Lohse, D. J.; Colby, R. H. In *Physical Properties of Polymers Handbook*; AIP Press: Woodbury, New York, 1996; Chapter 24, p 335.
(20) Jeon, H. S.; Lee, J. H.; Balsara, N. P.; Newstein, M. C. *Macromolecules* **1998**, *31*, 3340.
(21) Zin, W. C.; Roe, R. J. *Macromolecules* **1984**, *17*, 183.
(22) Roe, R. J.; Zin, W. C. *Macromolecules* **1984**, *17*, 189.
(23) Cohen, R. E.; Ramos, A. R. *Macromolecules* **1979**, *12*, 131.
(24) Bates, F. S.; Maurer, W.; Lodge, T. P.; Schulz, M. F.; Matsen, M. W. *Phys. Rev. Lett.* **1995**, *75*, 4429.
(25) Jackson, C. L.; Sung, L.; Han, C. C. *Polym. Eng. Sci.* **1997**, *37*, 1.
(26) Leibler, L. *Makromol. Chem., Rapid Commun.* **1981**, *2*, 393.
(27) Broseta, D.; Fredrickson, G. H. *J. Chem. Phys.* **1990**, *93*, 2927.
(28) Holyst, R.; Schick, M. *J. Chem. Phys.* **1992**, *96*, 7728.
(29) Balsara, N. P.; Jonnalagadda, S. V.; Lin, C. C.; Han, C. C.; Krishnamoorti, R. *J. Chem. Phys.* **1993**, *99*, 10011.
(30) Lin, C. C.; Jonnalagadda, S. V.; Balsara, N. P.; Han, C. C.; Krishnamoorti, R. *Macromolecules* **1996**, *29*, 661.
(31) Balsara, N. P.; Lin, C. C.; Hammouda, B. *Phys. Rev. Lett.* **1996**, *77*, 3847.
(32) Lin, C. C.; Jeon, H. S.; Balsara, N. P.; Hammouda, B. *J. Chem. Phys.* **1995**, *103*, 1957.
(33) Lin, C. C.; Jonnalagadda, S. V.; Kesani, P. K.; Dai, H. J.; Balsara, N. P. *Macromolecules* **1994**, *27*, 7769.
(34) Jeon, H. S.; Lee, J. H.; Balsara, N. P.; Majumdar, B.; Fetters, L. J.; Faldi, A. *Macromolecules* **1997**, *30*, 973.
(35) Leibler, L. *Makromol. Chem. Macromol. Symp.* **1988**, *49*, 1.
(36) Wang, Z. G.; Safran, S. A. *J. Phys. (Fr.)* **1990**, *51*, 185.
(37) Rachapudy, H.; Smith, G. G.; Raju, V. R.; Graessley, W. W. *J. Polym. Sci., Polym. Phys. Ed.* **1979**, *17*, 1211.
(38) Morton, M.; Fetters, L. J. *Rubber Chem. Technol.* **1975**, *48*, 359.
(39) Balsara, N. P.; Lohse, D. J.; Graessley, W. W.; Krishnamoorti, R. *J. Chem. Phys.* **1994**, *100*, 3905.
(40) Hammouda, B. *Adv. Polym. Sci.* **1993**, *106*, 87.
(41) de Gennes, P. G. *Faraday Discuss. Chem. Soc.* **1979**, *68*, 96.
(42) Rhee, J.; Crist, B. *J. Chem. Phys.* **1993**, *98*, 4174.
(43) Graessley, W. W.; Krishnamoorti, R.; Balsara, N. P.; Fetters, L. J.; Lohse, D. J.; Schulz, D. N.; Sissano, J. A. *Macromolecules* **1993**, *26*, 1137.
(44) Bates, F. S.; Rosedale, J. H.; Fredrickson, G. H. *J. Chem. Phys.* **1990**, *92*, 6255.
(45) Bates, F. S.; Rosedale, J. H.; Bair, H. E.; Russel, T. P. *Macromolecules* **1989**, *22*, 2557.
(46) Winey, K. I.; Gobran, D. A.; Xu, Z.; Fetters, L. J.; Thomas, E. L. *Macromolecules* **1994**, *27*, 2392.
(47) Perahia, D.; Vacca, G.; Patel, S. S.; Dai, H. J.; Balsara, N. P. *Macromolecules* **1994**, *27*, 7645.
(48) Fredrickson, G. H.; Helfand, E. *J. Chem. Phys.* **1987**, *87*, 697.
(49) Rangarajan, P.; Register, R. A.; Fetters, L. J.; Bras, W.; Naylor, S.; Ryan, A. J. *Macromolecules* **1995**, *28*, 4932.
(50) Certain equipment and instruments or materials are identified in this paper in order to adequately specify the experimental details. Such identification does not imply recommendation by the National Institute of Standards and Technology, nor does it imply the materials are necessarily the best available for the purpose.

MA9709718